Water Practice & Technology Vol 16 No 2
doi: 10.2166/wpt.2021.014

Treatment of AMD using a combination of saw dust, bentonite clay and phosphate in the removal of turbid materials and toxic metals

I. O. Ntwampe[a,b]

[a] Improves Lifes & Environ Foundation, Broadacres, Johannesburg, South Africa

[b] Department of Chemical Engineering, University of Johannesburg, Doornfontein 2028, Johannesburg, South Africa

E-mail: ontwampe@gmail.com

Abstract

Acid mine drainage collected from the western decant in South Africa was treated in a series of small-scale laboratory experiments. 200 mL of the sample was poured into five 500 mL glass beakers using flocculants formed by mixing size-optimized 1.5 g of bentonite clay with 3.5 g saw dust and 1.0 g of Na_3PO_4 in triplicates (experiment A). Four similar sets of control experiments were conducted using the same amount of bentonite clay and saw dust with varying Na_3PO_4, contents in AMD treatment; the rationale being to determine the efficiency of Na_3PO_4 (experiments B, C and D). The results show that conductivity has an influence in the removal of the turbid materials. The removal efficiency of toxic metals using a flocculant containing 220 μm bentonite clay particle size and 0.012 or 0.25 M of Na_3PO_4 is higher than 96% when compared to that of the samples dosed with a flocculant containing 0.05 M Na_3PO_4, which is less than 91%. The flocculant also showed optimal removal efficiency of both turbid materials and toxic metals, i.e. removal efficiency within a range 96.5–99.3%. The flocculants containing 0.025 M Na_3PO_4 showed optimal removal efficiency of turbidity, colour, toxic metals and natural organic compounds.

Key words: AMD, clay, flocculants, mixing, toxic metals

Highlights

- Effect of Na_3PO_4 in a flocculant.
- Adsorption efficiency of clay.
- Turbidity removal using synthetic flocculant.
- Removal of toxic metal using synthetic flocculant.
- Effect of saw dust in the removal of pollutants.

INTRODUCTION

South Africa is one of the countries rich in mineral resources such as gold, coal, uranium, steel and diamond. More than 60 percent of these minerals constitute acid mine drainage (AMD), an effluent generated from both operating and ceased mining sites. The acid state of the effluent is prone to dissolution of toxic metals and other soluble materials, which are detrimental to humans, organisms and aquatic life. Just as industrial wastewater is normally purified and re-used for essential or auxiliary processes, AMD can be treated through physico-chemical immobilization of toxic metals employing

Water Practice & Technology Vol 16 No 2
doi: 10.2166/wpt.2021.014

effective techniques. All types of contaminants present in wastewater can be treated according to their physico-chemical properties; that is, metabolization or decomposition of organic materials whereby metals transformed from labile toxic to form a more inert insoluble state which also exists in a less bio-available form in order to abate their detrimental effect (Nzihou & Sharrock 2009). A selection of cost-effective technology and a reagent(s) is imperative to encourage the mining authorities to employ such an approach of treating decanting AMD. However, a serious challenge associated with a majority of modern technologies includes high capital and operating costs (Ahmed *et al.* 2016; Fu *et al.* 2017), including difficulties encountered in the removal of toxic metals (Johnson & Hallberg 2003). A lot of studies conducted by Geldenhuys *et al.* (2001); Maree *et al.* (2004) and Petrik *et al.* (2003) revealed that most of the technologies characterized by high efficiency are sophisticated and costly. Research studies continued to explore some other mixed technologies, but the problem associated with costs still remains a challenge (Gitari *et al.* 2006, 2011; Nermen *et al.* 2009; Buzzi *et al.* 2011; Kopf *et al.* 2013). It was after various methods involving commercial reagents and new technologies showed unsuccessful outcomes that some other types of reagents such as waste materials and natural resources were investigated. The main problem regarding treatment of AMD is attributed to its complex chemical composition attributed to inorganic matter, dissolved and suspended solids, colour-and odour-producing materials and humic substances. Clay minerals and biomass were some of the techniques that were investigated using AMD and other synthetic complex wastewaters, where a majority of techniques exhibited high efficiency in the removal of contaminants (Tahir & Naseem 2007; Wei *et al.* 2008; Waanders & Brink 2010; Ntwampe *et al.* 2015a). The technique employed in this study includes treatment of the AMD using a combination of Na_3PO_4, bentonite clay and saw dust (flocculant). An advantage associated with this flocculant is that each reagent was added in reduced weight percentage (m/m %), thus reducing the cost for commercial coagulants or reagents and plausible detrimental effect when the dosage of each reagent exists in a pure form (Ntwampe & Moothi 2018). An advantage of using clay in this study is based on its materials, which are mostly composed of heterogeneous mineral mixtures (Bloch & Hutcheon 1992), taking into account that South African bentonite clay contains both calcium and magnesium montmorillonite mineral, affording it optimal exchange capacity and adsorption (Syafalni Abdullah *et al.* 2013; Nel *et al.* 2014). Bentonite clay also has very reactive constituents, which provide it with net negative charge (Oladipo & Gazi 2014).

The selection of saw dust is based on the adsorption capacity due to the presence of lignocellulose, a combination of lignin, cellulose, hemicelluloses, which constitutes the primary structure of the plant wall protecting against attack from microbes and animals (Zhao *et al.* 2012). Its morphological structure provides an adsorption capacity when pulverized to establish a large surface area. On the other hand, the selection of Na_3PO_4 is based on its ability to react with multivalent cations and convert them into insoluble compounds, particularly orthophosphates. Various hydrogen and dihydrogen phosphates have been investigated to determine the reaction mechanism between soluble phosphate and metal ions, and the results showed easy formation of insoluble metal phosphate salts (Nriagu 1984). Na_3PO_4 was selected among other phosphates because of low costs and low reactivity of the sodium component compared to other components such as potassium, ammonium and tri-hydrogen. The larger amount of Pb normally reacts with PO_4^{2-} to form hydrargyrite ($Pb_5(PO_4)_3Cl$), a species linked to phosphate occurring during a reaction within a wide pH range. Notwithstanding its existence in a wide pH range, it can be soluble in an acidic medium, depending on the stability and the concentration of reactive metals/substances in the medium (Amrah-Bouali *et al.* 1994). The outer surface of hydrargyrite is negative in a basic medium and positive in an acidic medium; substitution is ubiquitous, particularly for apatite chemistry, whereby a variety of ions may be attached to the apatite structure.

The objective is to investigate the efficiency of a flocculant (saw dust, size-optimised bentonite clay and Na_3PO_4 at reduced mass % (v/v %). The rationale being to optimise both the dosage and particle size of bentonite clay. The cost-effectiveness of a flocculant is the comparison between calculated

Water Practice & Technology Vol 16 No 2
doi: 10.2166/wpt.2021.014

costs to those obtained by Maree (1992). The reason to use cost analysis on the observations obtained by Maree (1992) with that obtained in this study was to optimize the system as the objectives are convergent; it also investigates cost-effective reagents which can replace costly conventional reagents. The novelty in this study is the use of natural and waste materials and low dosage of Na_3PO_4 without pre-processing of the reagents: a cost-saving approach.

MATERIALS AND METHODS

In this study, the coagulation-flocculation treatment was applied to the AMD sample using 1.5 g clay (bentonite), 10, 20, 30, 40, 50 and 60 mL of 4.5 g/L of $NaPO_4$, and 3 g/L saw dust dosages respectively. Another set of experiments was conducted with a dosage of a flocculant consisting of the same reagents added to the AMD sample. The experiments were conducted in triplicate for reproducibility. The AMD samples were treated using a jar test at 250 rpm for 2 min and then at 100 rpm for 10 min. The samples were allowed to settle for 1 h, after which the pH, electrical conductivity (EC), turbid materials (turbidity), toxic metals content, dissolved oxygen (DO), and oxidation reduction potential (ORP) were measured.

The AMD was collected from the Western decant in Krugersdorp (SA) in a 25 L plastic drum, and modified by blending it with kitchen wastewater to introduce organic materials. The overall pH, conductivity, DO, ORP and turbidity of the composite AMD solution were 2.56, 4.43 mS/cm, 234 mV, 4.1 mg/L and 213 NTU. The concentration of turbid materials of the AMD (9.2 g/200 mL) was measured by filtering a 200 mL of the sample on a filter of a certain mass using a high vacuum filter and the residue dried in an oven at 110 °C for 4 h, and the toxic metals content in the AMD sample is listed in Table 1.

Table 1 | ICP-OES results of the untreated AMD sample

Element	Conc^n (ppm)
Al	4.22
Ca	182.7
Co	8.336
Cu	14.45
Fe	27.2
K	6.89
Mg	141.2
Mn	30.7
Na	52.1
Ni	7.554
Pb	17.71
As	14.61
Cr	17.734
Zn	12.564

Bentonite clay was obtained from the Yellowstar Bentonite mine, a bentonite mining and supplying company situated in Parys in the Free State (SA). It was pulverised to 180 and 220 μm to an optimised and cost-effective size in order to curtail costs associated with energy and milling.

Toluidine blue dye purchased from Sigma Aldrich (South Africa) was used for coloration of the AMD; the rationale being to determine removal efficiency of colour using a flocculant employed in the study. 0.8 g of a dye was added to a litre of untreated AMD sample and stirred thoroughly.

Water Practice & Technology Vol 16 No 2
doi: 10.2166/wpt.2021.014

A stock solution was prepared using the quantities of the reagents (saw dust, bentonite clay and Na_3PO_4 filled to 1 L of demineralized water filled to a litre of volumetric flasks each to prepare a flocculant. The selection of 4.5 g/L Na_3PO_4 was used to determine the efficiency of the salt at low concentration for cost savings. The calculation of the mass of metal salts was used to obtain various concentrations of Na_3PO_4 (163.94 g/moL, basicity 2.23), No. 157750, Grade 97%.

Table 2 shows the metal salts dosed into the AMD samples.

Table 2 | Quantities of the clay, saw dust and Na_3PO_4 dosed to AMD sample

Salt	Mass (g)	Conc (mol/L)	M^{3+}conc (M)	MM (g/moL)
A-Na_3PO_4	8.2	0.05	0.05	163.9
A-Na_3PO_4	4.1	0.025	0.025	82.0
B-Na_3PO_4	2.05	0.012	0.012	41.0
Bentonite clay	1.5	0.005	0.005	540.5
Saw dust	1.5			–

Quality control

The utensils and experimental equipment were all rinsed three times using distilled water; the electrodes used were also thoroughly rinsed using distilled water. The samples were analysed at North-West University (SA). All equipment used for the experiments were calibrated as per laboratory standards, and the ICP-OES, XRD, and SEM analyses were conducted by qualified technicians. All the instruments were calibrated on a daily basis using appropriate standard solutions.

Jar tests

The equipment used for the jar tests was a BIBBY Stuart Scientific Flocculator (SW1 model), which has six adjustable paddles with rotating speeds between 0–350 rpm. A 200 mL sample of AMD (containing 9.3 g of turbid materials as measured by filtering 200 mL of the AMD sample, dehydrating it using an oven at 60 °C for 4 hours, and thereafter measuring the mass) was poured into each of the five 500 mL glass beakers for the test.

A Merck Turbiquant 3,000T Turbidimeter (Japan) was used to determine turbid materials (turbidity) in the supernatant, using NTU as a unit of measure. It was calibrated with 0.10, 10, 100, 1,000, and 10,000 NTU standard solutions. Turbidity was calculated by NTU conversion; that is, by multiplying the turbidity readings by 3.42.

The pH, EC, DO and ORP were measured using a SensoDirect Multimeter (South Africa) with an electrode filled with silver chloride solution and the outer glass casing with a small membrane covering the tip. The equipment was calibrated with standard solutions at pH of 4.0 and 7.0 before use. Parameters were measured using their respective probes, and the instrument was fitted with a 'temperature correction' device.

DOC, UV254 and SUVA

Organic and NOM loading present in the sample was determined by filtering the samples through a 0.45 μm membrane carbon filter. The concentration of total dissolved solids (TSS) was measured by TOC analyzer as 3.4 mg/L after 0.45 μm Millipore filtration; and was kept air-tight and stored at room temperature; UV254 and DOC measurements were taken using a spectrophotometer (Agilent

Water Practice & Technology Vol 16 No 2
doi: 10.2166/wpt.2021.014

Technologies Cary 60 UV-Vis) and a Shimadzu TOC-L analyser, respectively. Standard carbon solutions of 1, 5, 10, 20 and 30 mg/ℓ were prepared using potassium hydrogen phthalate (KHP) and de-ionised water to calibrate the instrument. Measurements were carried out in duplicate and the average of the results was used in the determination of the presence of humic and non-humic substances in the sample, specific ultraviolet absorbance (SUVA) values in ℓ/mg.m were determined as per Weishaar *et al.* (2003), as shown by Equation (1).

$$\mathrm{SUVA}_{\mathrm{rawAMD}} = \frac{UV_{254}}{TDS} \times 100 \tag{1}$$

EXPERIMENTAL PROCEDURES

Experiment A: 200 mL of a sample was poured into each of the five 500 mL glass beakers and dosed with a synthetic flocculant as mentioned, and treated in a jar test. The sample was allowed to settle for 1 h, after which the pH, EC, turbid materials, DO, and ORP measurements were repeated.

Experiment B: A similar set of experiments, where a flocculant in 1 L of demineralized water was added to the AMD and treated in the same manner.

X-ray diffractometric analysis

The X-ray diffraction (XRD) patterns of the turbid materials (salts content) adsorbed onto the sludge of the AMD samples dosed with a flocculant were recorded using a Rigaku Miniflex II Desktop X-ray diffractometer (Japan) with Cu Kα radiation. A step size of 0.02° at a speed of 4° (2θ)/min over 10–80° was applied. The minerals in VM treated between 950 and 1,300 °C were quantified by Siroquant software.

Scanning electron microscopic analysis

A KYKY-EM3200 digital scanning electron microscope (SEM; model EM3200) (China) was used to produce the SEM photomicrographs.

Inductively coupled plasma (ICP-OES)

A Perkin Elmer Optima DV 7000 ICP-OES optical emission spectrometer (USA) was used to determine the concentration of metals and other pollutants in the supernatant of the AMD samples. The measurements were conducted by a qualified technician in the chemistry department following the standard operating procedure of the ICP-OES equipment.

Adsorption capacity

Pseudo-second order model was applied in adsorption experiments to determine kinetic study of adsorption capacity of an adsorbate onto adsorbent; that is, turbidity onto the flocculant consisting of a combination of bentonite clay, saw dust and Na_3PO_4. The Freundlich model was applied for multilayer adsorption of turbidity on a surface of a heterogeneous adsorbent. Only the pseudo-second order model and Freundlich were selected based on the application and limited graphs required.

Water Practice & Technology Vol 16 No 2
doi: 10.2166/wpt.2021.014

Pseudo second order model

$$\frac{dq_t}{dt} = k_2(q_e - q_t)^2 \quad (2)$$

where q_e is the adsorbed amount of the turbid materials at equilibrium (mg/g), q_t is the adsorbed amount of turbid materials at a certain time t (mg/g) and k_2 is the rate constant for the second order adsorption kinetics, as calculated from the slopes of the plots ln ($1\text{-}q_t/q_e$) versus t and ($i/q_t - 1/q_e$) versus $1/t$.

Freundlich isotherm

The linearized Freundlich equation is represented as:

$$\log q_e = \log K_F + \frac{1}{n}\log C_e \quad (3)$$

where K_F and n are equilibrium constants and adsorption intensity respectively.

A plot of log q_e vs log C_e should be linear if the model fits the experimental data.

RESULTS AND DISCUSSION

The experimental results show the efficiency of a flocculant consisting of bentonite clay, saw dust and Na_3PO_4 at a low molar % (m/m%) exhibits high performance for the removal of toxic metals from the AMD sample. The concentration of the AMD sample was of a complex nature in order to elevate reactivity rate after the dosage with a flocculant characterized by porosity, ionic exchange, intercalation, selectivity and sorption. The performance of a reagent in the removal of toxic metals was typically influenced by the EC and ionic strength attributed to the complexity of the sample, both determining the destabilization-hydrolysis process, resulting in high adsorption capacity. The relationship of the ionic strength (I) of a colloidal suspension and the valence (Equation (4)) shows optimal removal efficiency based on the ionic strength (i) and the concentration (c).

$$I = 0.5\left(\sum c_i z_i^2\right) \quad (4)$$

where I is the ionic strength, c is the molar concentration of ion and z is the valence.

The determination of the ionic strength of the colloidal suspension can be experimentally or theoretically calculated using Equation (4). In this study, ionic strength was calculated due to a lack of the measuring equipment, and the results are shown in Table 3.

Table 3 | Ionic strength of the reagents dosed in the AMD during treatment

Reagents	Ionic strength (M)
0.050 M Na_3PO_4	0.20
0.025 M Na_3PO_4	0.1
0.012 M Na_3PO_4	0.05

The effectiveness of a treatment process is shown by the rate of deprotonation during destabilization, which correlates with the hydrolysis, leading to the rate of adsorption (Ntwampe *et al.* 2013a). Figure 1 illustrates the relationship between the pH and the EC or DO as the function of

Water Practice & Technology Vol 16 No 2
doi: 10.2166/wpt.2021.014

the dosage employed during AMD treatment using a combination of clay, saw dust and (0.012, 0.025 and 0.05 M) of Na_3PO_4 in a flocculant.

The pH of the samples with a flocculant containing a dosage of 0.012, 0.025 and 0.05 M Na_3PO_4 dosage exhibited an inconsistent changing trend from 2.56 to the ranges of 2.62–2.4, 2.63–2.17 and 2.41–2.20 respectively (Figure 1). Such a changing pattern may be attributed to perturbation occurring between forward and reverse reactions. The pH and the EC of the samples dosed with a flocculant containing 0.012 M Na_3PO_4 show a correlation. On the contrary, the pH and the EC of the samples dosed with a flocculant containing 0.025 and 0.05 M Na_3PO_4 do not show correlation (Figure 1); that is, the EC shows an inconsistent changing trend. However, the high ionic strength of a solution (Table 3) is indicative of effective destabilization-hydrolysis. Notwithstanding the changing trend of the EC, the neutralizing effect of $CaCO_3$ is effective as the pH decreases consistently.

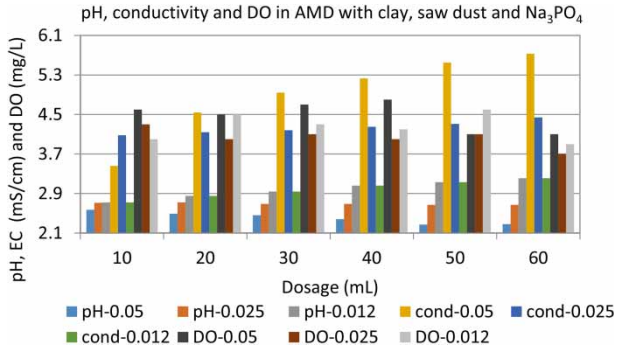

Figure 1 | pH, conductivity and DO of AMD sample with varying dosage of clay, saw dust and Na_3PO_4.

The DO of samples dosed with the flocculants containing 0.012, 0.025 and 0.05 M Na_3PO_4 changed from 4.1 mg/L (untreated AMD) to the ranges of 4.2–4.8, 4.1–5.7 and 2.1–4.6 mg/L respectively. The low DO range shown by the samples dosed with a flocculant containing 0.05 M Na_3PO_4 is probably attributed to high rate of oxidation of the cations contributing to high conductivity. This is exhibited by a low DO and conductivity of the samples dosed with a flocculant containing 0.012 M Na_3PO_4. The concentration of the Ca in the raw AMD (Table 1) was reduced from 188 to 59 ppm (Table A1, Supplementary material), and the removal is presumably through adsorption onto the flocs, co-precipitation or enmeshment in the precipitates (Moore *et al.* 1978). The pH, EC, DO, ORP, and turbid materials measurements of the 1.5 g of bentonite clay in a litre of demineralized water, are shown in Table 4. The metal concentrations of the untreated AMD are shown in Table 1.

Table 4 | Properties of the clay and AMD sample

Sample	pH	Conductivity (mS/cm)	TTTSS (g/L)	DO (mg/L)	ORP (mV)
Clay	2.15	2.66	13.6	5.8	230
Raw AMD	2.52	4.30	105	3.9	236

The EC of the samples dosed with a flocculant containing 0.05, 0.025 and 0.012 M Na_3PO_4 (Figure 1) changed from 4.30 mS/cm (untreated AMD) to the ranges 5.09–7.66, 2.43–4.34 and 3.15–4.24 mS/cm respectively. On the other hand, AMD samples with 40–60 mL of 0.05 M Na_3PO_4 dosage exhibit an inconsistent changing pattern; only the samples dosed with a flocculant containing 0.025 M Na_3PO_4 exhibited a uniform decreasing pattern. The oxidation reduction potential (ORP) (Figure 2), is an indication of the rate at which redox occurs on the metals to form cationic and anionic metal; these are highly reactive compared to the parent molecule and indicative of the

Water Practice & Technology Vol 16 No 2
doi: 10.2166/wpt.2021.014

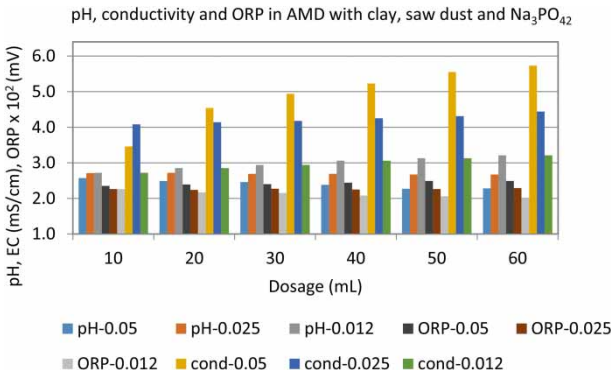

Figure 2 | pH, conductivity and ORP of AMD sample with varying dosage of clay, saw dust and Na_3PO_4.

formation of precipitates which are removed by co-precipitation or sorption. Settling time of 1 hour allowed optimal nucleation, crystallization and sedimentation (Ntwampe *et al.* 2013b), resulting in effective physico-chemical reaction, which is predominantly induced by Brownian motion to form fully fledged flocs. Figure 2 shows the pH, conductivity and ORP changing trend with dosage.

The ORP changed from 236 mV in the raw AMD sample to a range 227–268 mV in treated samples (supernatant). The ORP of raw AMD sample showed a changing trend from 236 mV to the redox potential, which is in a range −6–32 mV in treated samples. The results show a correlation between ORP and the dosage, whereas the samples dosed with a flocculant containing 0.012 M Na_3PO_4 has ORP in a range −6 and −0.2 mV, which indicates that all the samples went through the oxidation process. On the other hand, ORP of the samples dosed with flocculants containing 0.025 and 0.05 M Na_3PO_4 exhibited an inconsistent changing trend in a range 5–21 and 13–32 mV respectively, indicating that the reduction reaction was a predominant phenomenon, the latter changing trend showing a high reducing strength. Figure 3 shows the pH, ORP and residual turbid materials of the AMD samples with varying concentrations of Na_3PO_4 in the flocculant. The effectiveness of turbid materials removal ranges from 1.32 to 2.74 mg/L (75–97.1%).

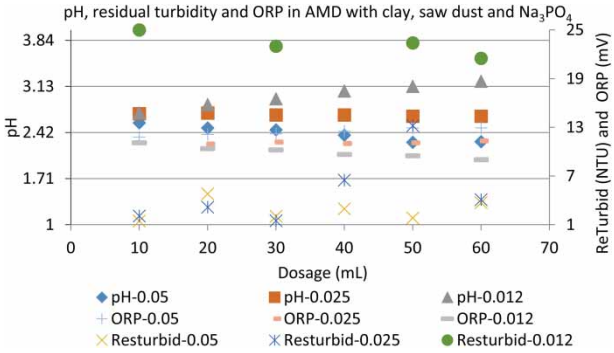

Figure 3 | pH, residual turbid materials and ORP of treated AMD sample dosed with varying concentration of Na_3PO_4 in the flocculant.

The residual turbidity of the samples dosed with the flocculants containing 20–50 mL of 0.05 M Na_3PO_4 shows an increasing trend in a range of 1.2–6.3 mg/L, a slightly lower than 10.4 NTU as shown by the sample dosed with a flocculant containing 60 mL. The samples dosed with a flocculant containing 0.025 and 0.012 M Na_3PO_4 exhibit an inconsistent lower residual turbidity showing a changing trend in the ranges of 2.43–4.34 and 15.3–4.1 mg/L respectively. Residual turbidity of a flocculant with 0.025 M Na_3PO_4 is lower than that of the samples dosed with the flocculants containing 0.012 and 0.05 M Na_3PO_4. Apart from the physical sorption mechanism of both bentonite clay and saw dust, destabilization-hydrolysis attributable to hydrated PO_4^{2-} played a pivotal role in optimal

Water Practice & Technology Vol 16 No 2
doi: 10.2166/wpt.2021.014

removal of the pollutants (Figure 3); including the transformation of toxic metals from a labile toxic form to more inert insoluble materials, which abated their bio-availability and harmful effects on the ecosystem. The ability of apatite to react easily with divalent and multivalent cations and metal ions resulted in the formation of insoluble orthophosphates and metal phosphate salts, which are stable and inactive to the geological environment (Suzuki *et al.* 1981, 1982, 1984). Another benefit associated with apatite is plausible replacement of OH^- ions by anions, which constitutes permanent hardness, including the effect of multiple layers that are more likely to behave like clay by reducing the amount of pollutants through ion exchange and intercalation. This suggests that sorption by apatite is identical to that of bentonite clay (Strawn & Sparks 1999; Azihou & Sharrock 2010). The products resulting from the dissolution of apatite in an acidic medium such as calcium cations and hydrogenophosphate are attributable to its high reaction rate and interactions with a variety of pollutants present in wastewater. Reactivity is also influenced by its hydrated form in solution where polar water molecule, partially negative and positive hydroxyl and hydrogen ions respectively. In a case where water molecules do not play a major role during sorption, dehydration takes place, allowing ionic exchange; a process which is influenced by the amount of enthalpy of hydration. Metal ions with low enthalpy of hydration are easily exchangeable compared to those with higher enthalpy, where the mass transfer rate becomes significant for ionic exchange and selectivity. The reaction which fastens the process is defined by rapid mass transfer whereas slow reaction by mass transfer resistance which is influenced by solid diffusion than surface or pore diffusion (Baillez *et al.* 2004). The removal efficiency of toxic metals shown by the results confirms previous observation (Nriagu 1984) stating that the PO_4^{3-} can react with toxic metals in a wide pH range to form insoluble metal phosphate precipitates. The conductivity of the samples with a flocculant containing 0.025 M Na_3PO_4 dosage falls between the conductivity of the samples with 0.012 or 0.05 M Na_3PO_4 dosage, hence yielding the residual turbid materials, which fall between them. The experimental results therefore show that there is a strong correlation between the pH, conductivity and turbid materials removal. The efficiency of the flocculant (Figure 3) using 0.12, 0.25 and 0.05 M of Na_3PO_4 in a flocculant is above 96%, the efficiency correlating to the observation of the study conducted by Ntwampe & Moothi (2019). On the other hand, the polarity of the bulk fluid also plays a pivotal role during wastewater treatment (Ntwampe *et al.* 2015a), citing the effect resulting from the cleavage of water molecules to form partially positive protons ($H^{\sigma+}$) and hydroxyl ($OH^{\sigma-}$) ions. The former partially suppresses the pH of a solution, whereas the latter takes part during hydrolysis and partial regulation of the pH in the system. Partially negative/positive ions act as ligands by attracting neighbouring cations/anions from the wastewater to segment the formation of settleable agglomerates. It is suggested that the $H^{\sigma+}$ and $OH^{\sigma-}$ can polarize the octahedral hydrosphere around the central metal ions (M^{3+}) and undergo further hydrolysis (Equations (5) and (6)).

$$M - OH + H^+ \rightleftharpoons M - OH_2^+ \tag{5}$$

$$M - OH + OH^- \rightleftharpoons M{-}O^- + H_2O \tag{6}$$

Amphotericity of water is another parameter that plays a role during destabilization-hydrolysis (Equations (4) and (5)), which then revealed an insignificant role played by pH adjustment in wastewater treatment using a flocculant containing Na_3PO_4. It is essential to note that pH adjustment is mainly to reduce the solubility of toxic metals in a solution with minimal effect during destabilization-hydrolysis as a majority of coagulants react within a wide range of pH (Flynn 1984). As a matter of fact, the process depends predominantly upon the physico-chemical properties of the solution (Moore *et al.* 1978; Flynn 1984) and the reactivity rate (electronegativity, acidity and distance between the neighbouring colloidal particles (Ntwampe 2013; Ntwampe *et al.* 2013a; Ntwampe *et al.* 2015b).

Water Practice & Technology Vol 16 No 2
doi: 10.2166/wpt.2021.014

The flocculant showed optimal removal of toxic metals such as Co, Cu, Ni, Pb, As, Cr and Zn from 8.336, 14.45, 7.554, 17.71, 14.61, 8.434 and 12.564 ppm (Table 1) to 0.138, 0.144, 0.373, 0.189, 0.270, 0.795 and 0.315 ppm (Table A1) respectively. The removal efficiency of Pb corroborates with recorded observations (Nriagu 1984; Azihou & Sharrock 2010) by achieving the highest efficiency from 17.7 to 0.189, a removal efficiency of 98.9%. The observations show an immense mass transfer for various metal ions and considerable pore and surface diffusion through ion exchange at specific sites, and intercalation between the sheets formed by the reaction of hydroxyapatite, saw dust and bentonite clay. It is suggested that saw dust and ionized Na_3PO_4 firstly occupied the free sites on the surface of the bentonite clay to form new interfacial structures available for sorption and intercalation. Spontaneous dissolution-sorption mechanism cannot be considered as the only phenomenon attributable to optimal removal of turbidity; also hydration occurring around the central metals utilizes internal enthalpy of hydration to dehydrate aqueous metal prior to ionic exchange, which must be higher than the hydration enthalpy of adsorbable toxic metal ions. On the other hand, the dissolution-precipitation mechanism revealed that hydroxylapatite dissolves under a wide range of pH values and increases the mechanisms that govern the removal rate of toxic metal ions (Cheng *et al.* 1997), and such an inference is invoked by the results obtained in this study (Table A1). Some of the metals are largely removed compared to others, suggesting that the metals with higher enthalpy of hydration (Pb, Cu, Cr and As) exhibited optimal removal efficiencies. Removal efficiency is also influenced by surface and pore diffusion including intra-particle diffusion, which may at times be ineffective due to steadiness at room temperature. The efficiency of hydroxylapatite is also apparent when the metal ions precipitate due to low solubility on the surface of the hydroxylapatite during the secondary phase. Low removal efficiency of some toxic metals is more likely to be attributable to the interference of diffusion by clogging of the pathway during accumulation of amorphous products. Most of such metals are unstable at the primary stage, such as Cr^{2+} and Fe^{2+}, among others. In addition to sorption mechanisms, the performance of ionic exchange is influenced predominantly by the cation-exchange-capacity (CEC) occurring when the metals attach to the surface of the flocculant and pushes away more soluble indigenous calcium from the flocculant, most of which is attached to hydroxylapatite. Alternatively, calcium may dissolve first followed by phosphate ions, allowing precipitation of toxic metal ions by homogeneous (in solution) or heterogeneous (on the remaining solid hydroxylapatite) nucleation (Manecki *et al.* 2000a, 2000b). The final removal of toxic metals is likely to be attributed to the crystallinity, specific surface area, density, pH, temperature, ligands, concentration of the metals and addition rate, as they also form part of the physico-chemical properties of the system. The removal efficiency of Ca^{2+} and Mg^{2+} ions (Table A1) shows that a large amount reacted with PO_4^{2-} to form a new metal-phosphate species, which is invoked by the available observations revealed in the study conducted by Cheng *et al.* (1997). Figure 4 shows the relationship between the pH and the removal efficiency of turbid materials using a flocculant containing 0.025 M Na_3PO_4. It can therefore be concluded that pollutant removal (Figure 3) is attributed to attraction between adsorbent and adsorbate (chemosorption), and

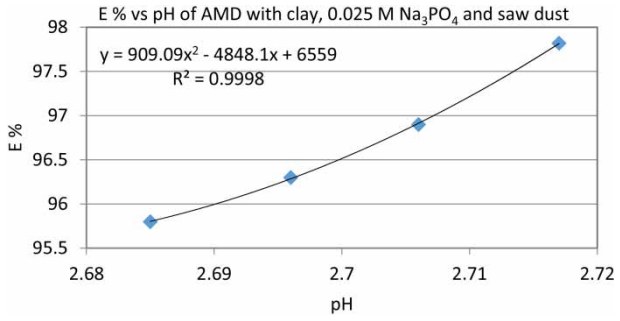

Figure 4 | Correlation between E% and varying concentrations of Na_3PO_4 in a flocculant of treated AMD.

Water Practice & Technology Vol 16 No 2
doi: 10.2166/wpt.2021.014

attraction by neighbouring oppositely-charged particles (physicosorption) induced by van der Waal's forces of attraction (Ntwampe *et al.* 2015c), ion exchange (Sinha *et al.* 2013), and electrostatic repulsions on the basal planes or covalent bonds by amphoteric ligands on the edge of montmorillonite with the functional (carboxyl) group (van der Watt 2011), including its large specific surface area and exchange capacity (Syafalni Abdullah *et al.* 2013). Figure 4 shows the relationship between the pH and removal efficiency of turbid material using a flocculant containing 0.025 M Na_3PO_4. The selection of the molarity was to investigate the performance of the flocculant using optimized dosage (0.025 M being between 0.012 and 0.05 M).

Figure 4 yielded a high correlation regression (R^2) of 99.9%, which is indicative of the accuracy of the experimental data used to plot the graph. Figure 5 is a Freundlich model showing a relationship between removal efficiency and the dosage of a flocculant containing 0.025 M Na_3PO_4. On the other hand, Figures A1 and A2 (Supplementary material) show the Freundlich model plotting a relationship between removal efficiency and dosage of a flocculant containing 0.05 M Na_3PO_4, and the pseudo-second order model showing the relationship between adsorption efficiency at equilibrium using a flocculant containing 0.025 M Na_3PO_4.

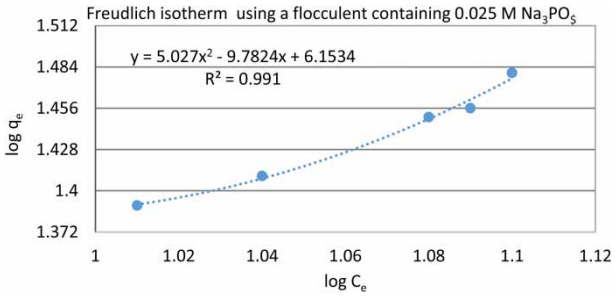

Figure 5 | Correlation between E% and ORP of the AMD using varying dosages of 0.05 M Na_3PO_4 in a flocculant.

The experimental data (using a flocculant containing 0.025 M Na_3PO_4) used to plot a graph shows a best mathematical fit for Freundlich adsorption isotherms; with correlation regression of 0.998 (99.8%). On the other hand, the experimental data using a flocculant containing 0.05 M Na_3PO_4 (Figure A1) also shows a best fit with correlation regression of 0.993. The experimental data (using a flocculant containing 0.025 M Na_3PO_4) used to plot a graph (Figure A2) shows a best mathematical fit for pseudo-second order with coefficient regression (R^2) of 0.999. Figure 6 illustrates the mineral compounds of the treated AMD with bentonite clay, saw dust and 0.025 M Na_3PO_4 dosage.

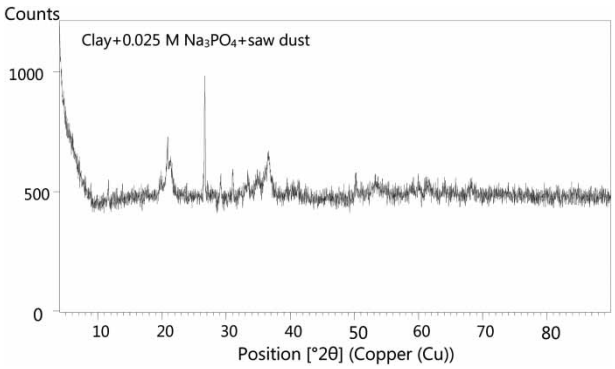

Figure 6 | XRD of treated AMD with 0.025 M Na_3PO_4 in a flocculant.

The XRD curves (Figure 6), where the AMD sample treated with a flocculant containing 0.025 and particle size 180 μm (bentonite clay) showed two peaks representing crystalline materials at 2θ

Water Practice & Technology Vol 16 No 2
doi: 10.2166/wpt.2021.014

positions of 20° and 37° respectively, with an intensity of 500 counts. The narrow diffraction peaks between 400 and 500 counts are indicative of the presence of trace metals disorderly stacked up by flocs. The XRD pattern of such minute peaks representing trace metals (Figure 6) confirms a high efficiency using that particular flocculant. SEM micrographs (Figure 7) show the results of the AMD sample dosed with a flocculant containing 0.025 and 0.05 M Na_3PO_4, and particle size of 220 μm during rapid mixing. On the other hand, Figure A3 shows the sludge of the sample dosed with a flocculant containing 0.025 and 0.05 M Na_3PO_4, and particle size of 220 μm during rapid mixing

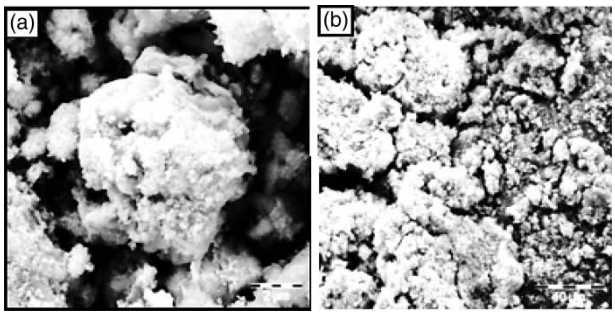

Figure 7 | SEM micrographs of treated AMD with a flocculant containing 0.025 Na_3PO_4.

The SEM micrograph of the sludge of a sample dosed with a flocculant containing 0.05 M Na_3PO_4 (Figure 7(a)) shows scattered dense flocs surrounded by a cluster of small flocs, indicating rapid floc formation due to over-dosage, which resulted in agglomeration of a dense sponge-like structure surrounded by large voids and smaller agglomerates. On the other hand, the SEM micrograph of a sample dosed with a flocculant containing 0.025 M Na_3PO_4 showed normal dispersed uniform-sized flocs joined together, an indication of a steady rate of sorption due to optimally pulverised bentonite clay with large surface area. The micrograph shows a normal distribution of saw dust and Na_3PO_4 particles throughout the surface of the clay to form a rigid adsorbent. SEM microgram sample dosed with a flocculant containing 0.025 and 0.05 M Na_3PO_4, and particle size 220 μm during rapid mixing (Figure A2), shows almost identical crystal morphology; that is, large flocs with perforated surface joined together by small flocs. It is suggested that the morphology of the micrographs is attributed to high sorption capacity of the pollutants by permanent negative surface charge and interlayer spaces resulting predominantly in higher ion exchange capacity and metal sorption, an observation already determined by Abbas *et al.* (2018); Chen *et al.* (2018); Delavernhe *et al.* (2015) and Khandelwal *et al.* (2019). Based on the constituents of bentonite clay, saw dust and chemical composition of Na_3PO_4, it is conceivable to suggest that optimal removal of the pollutants is dependent upon a large number of pores and abundant surface functional groups (Figure A2), utilized in metal adsorption. The tiny voids distributed throughout the micrograph and clustered morphological structure are indicative of high sorption capacity. Based on the high performance exhibited by the bentonite clay with 220 μm particle sizes, excessive milling using high energy consumption is costly and unnecessary, as larger particle size using low energy consumption during milling yields identical results.

The Pearson correlation coefficient (r) was employed to calculate the relation between pH and residual turbidity of the AMD sample dosed with a flocculant. According to the correlation coefficient, 0.70 or higher is a very strong relationship, 0.40–0.69 is a strong relationship, and 0.30–0.39 is a moderate relationship. The experimental results used for the Pearson model are duplicate pH and residual turbid materials parameters of the AMD sample dosed with a flocculant containing 0.025 M Na_3PO_4, where exp (A) represents residual turbidity of the sample with particle size 180 μm (bentonite clay), whereas exp (B) represents residual turbidity with particle size 220 μm;

Water Practice & Technology Vol 16 No 2
doi: 10.2166/wpt.2021.014

and the model is represented as follows:

$$\Sigma x_{exp(A)} = 11.15,\ \ \Sigma x^2_{exp(A)} = 24.87, \Sigma y_{exp(A)} = 11.28, \Sigma y^2_{exp(A)} = 25.45 \text{ and } \Sigma xy_{exp(A)} = 25.15 \quad (7)$$

$$\Sigma x_{exp(B)} = 10.76, \Sigma x^2_{exp(B)} = 23.16, \Sigma y_{exp(B)} = 11.54, \Sigma y^2_{exp(B)} = 26.64 \text{ and } \Sigma xy_{exp(B)} = 24.83 \quad (8)$$

The r-value obtained for the AMD samples (exp. A) in experiment (A) is 0.65 (65%) with the range of the correlation coefficient from −1 to 1. The r-value obtained for the AMD sample (exp. B) in experiment (B) is 0.55 (55%), showing a strong relationship. That is validated by the correlations of the samples dosed with a flocculant containing 0.025 and 0.05 M Na_3PO_4. The determination of natural organic matter (NOM) has not been a popular measurement in water treatment processes; however, it is significant as a majority of NOM consists of humic (hydrophobic) and fulvic (hydrophilic) acids such as high and low molecular weight compounds. These compounds are harmful to treated water, particularly when it has to be distributed for potable supplies and critical industrial activities (drinking, cleaning laboratory equipment, food production, etc.) as they react with disinfectant to form disinfection by-products (DBPs) (drinking, cleaning laboratory equipment, food production, etc.) (Chowdhury 2013). A sample of treated effluent dosed with a flocculant containing 0.025 Na_3PO_4 and particle size 220 μm (clay) was assessed to determine the amount of NOM (turbidity) at equilibrium employing the UV_{254} technique. Adsorbable turbid materials remaining after coagulation could not be adsorbed due to equilibrium state with adsorbed turbid materials onto the flocs (Figure A4). The correlation regression of both the SUVA and UV254 are high, at 0.958 and 0.967 respectively ($p > 0.05$); high SUVA R2 shows optimal removal efficiency of NOM and TOC using a flocculant containing 0.025 Na_3PO_4 and particle size 220 μm.

CONCLUSION

The principal objective of this study was to determine the efficiency of a flocculant consisting of bentonite clay, saw dust and Na_3PO_4 in the removal of turbid materials present in the AMD sample. The reagents which were used to prepare a flocculant (bentonite clay, saw dust and Na_3PO_4) were mixed and dosed directly without processing as stated. The experimental results revealed that a combination of bentonite clay, saw dust and 0.012 and 0.025 M Na_3PO_4 without pre-processing yielded optimal removal of turbid materials, colour, NOM and toxic metals. The removal efficiency is indicative of a complete and effective destabilization-hydrolysis, a phenomenon that is indicated by the removal efficiency of the pollutants. The presence of Na_3PO_4 in a flocculant shows significant contribution in the removal of Ca and Mg from the AMD, which also acts as an ideal water softening agent. Bentonite clay and saw dust showed optimal removal of the turbid materials due to their porous and ion-exchange properties. On the other hand, the phosphate component of the flocculant shows optimal removal of the divant metals due to its ability to react with most of the metals and metalloids, such as Na, Mn and Fe. In addition, optimal removal efficiency associated with porosity and ionic exchange is an indication of adsorption of the pollutants through physico-chemical phenomenon. The flocculant, consisting of 0.025 M Na_3PO_4 and bentonite clay of 220 μm particle size, showed optimal removal efficiency of toxic metals and colour; that is, higher than 96%. The observation shows that optimization of the flocculant using Na_3PO_4 and particle size of the bentonite clay is significant for the removal of pollutants in the wastewater. Proliferation of electrical conductivity with dosage (increasing ionic strength of a solution) corresponds to optimal sorption of pollutants; this indicates that electrical conductivity plays a pivotal role during destabilization-hydrolysis. Optimal removal of pollutant still occurred using moderate particle size; this shows that over-pulverization of the reagents is unnecessary and costly. Optimal removal of NOM is indicative of their reactivity during

Water Practice & Technology Vol 16 No 2
doi: 10.2166/wpt.2021.014

physico-chemical reactions; that is an indication of their catalytic property during the treatment process. The SEM micrographs of the flocculants containing 0.025 and 0.05 M or 180 and 220 μm particle size all show dense sponge-like flocs surrounded are costly and unnecessary; bigger particle size (220 μm) yielded identical removal efficiency of pollutants as smaller particle size. The clusters exhibited by the sludge of treated samples (SEM micrographs) are indicative of high adsorption capacity of the adsorbent, and a high removal of the pollutants using moderate pulverised bentonite clay (220 μm). The bill of material (reagents) used in the treatment of 15 ML of the AMD amounts to R 33.3 (US$ 1.85) (Table A4), excluding labour costs; this is less compared to the costs obtained by Maree (1992). The practical interpretation of this comparison indicates that cost reduction on water treatment chemicals can be achieved by employing a mixture of commercial reagent(s) with waste materials with high sorption capacity.

DATA AVAILABILITY STATEMENT

All relevant data are included in the paper or its Supplementary Information.

REFERENCES

Abbas, Z., Ali, S., Rizwan, M., Zaheer, I. E., Malik, A., Riaz, M. A., Shahid, M. R., Rehman, M. Z. U. & Al-Wabel, M. I. 2018 A critical review of mechanisms involved in the adsorption of organic and inorganic contaminants through biochar. *Arabian J. of Geosci.* **11**(16), 448. https://doi.org/10.1007/s12517-018-3790-1.

Ahmed, S., Ahmad, M., Swami, B. L. & Ikram, S. 2016 A review on plants extract mediated synthesis of silver nanoparticles for antimicrobial applications: a green expertise. *J. of Adv. Res.* **7**(1), 17–28.

Amrah-Bouali, S. R., Rey, C., Lebugle, A. & Bernache, D. 1994 Surface modification of hydroxyapatite ceramic in aqueous media. *Biomaterials* **15**(4), 269–272.

Azihou & Sharrock, P. 2010 Role of phosphate in the remediation and reuse of heavy metals polluted wastes and sites. *Waste Biomass Valor.* **1**, 163–174.

Baillez, S., Nzihou, A., Beche, E. & Flamant, G. 2004 Removal of lead (Pb) by hydroxyapatite aorbent. *Proc. Safety Environ. Proctec.* **82**(2B), 175–180.

Bloch, J. & Hutcheon, I. E. 1992 Shale diagenesis: a case study from the Albanian harmon member (Peace river formation), western Canada. *Clays and Clay Min.* **40**(6), 682–699.

Buzzi, D. C., Viegas, L. S., Silvas, F. P. C., Espinosa, D. C. R., Rodrigues, M. A. S., Bernardes, A. M. & Tenório, J. A. S. 2011 The use of microfiltration and electrodialysis for treatment of acid mine drainage. *Int. Mine. Wat. Ass.* 286–290.

Chen, H., Xie, A. B. & You, S. H. 2018 A Review: Advances on Absorption of Heavy Metals in the Waste Water by Biochar. In *5th Annual International Conference on Material Science and Environmental Engineering (Msee 2017)*, p. 301

Cheng, X., Wright, J. V., Conca, J. L. & Perrung, L. M. 1997 Effects of pH on heavy metal sorption on mineral apatite. *Environ. Sci. Tech.* **31**(3), 624–631.

Chowdhury, S. 2013 Trihalomethanes in drinking water: effect of natural organic matter distribution. *Water SA* **39**(1), 1–8.

Delavernhe, L., Steudel, A., Darbha, G. K., Schäfer, T., Schuhmann, R., Wöll, C., Geckeis, H. & Emmerich, K. 2015 Influence of mineralogical and morphological properties on the cation exchange behavior of dioctahedral smectites. *Colloids and Surfaces A: Physicochem. and Eng. Aspects* **481**, 591–599.

Flynn, C. M. 1984 Hydrolysis of inorganic iron(III). *J. of Am. Chem. Soc.* **84**, 31–41.

Fu, R., Zhang, X., Xu, Z., Guo, X., Bi, D. & Zhang, W. 2017 Fast and highly efficient removal of chromium (VI) using humus-supported nanoscale zero-valent iron: influencing factors, kinetics and mechanism. *Sep. and Purif. Technol.* **174**, 362–371.

Geldenhuys, A. J., Maree, J. P., Fourie, W. J., Smit, J. J., Bladergroen, B. J. & Tjati, M. 2001 Acid mine drainage treated electrolytically for recovery of hydrogen, iron(II) oxidation and sulphur production. In: *Submission at the 8th International Congress on Mine Water & Environment in Johannesburg*, South Africa.

Gitari, M. W., Petrik, L. F., Etchebers, O., Key, D. L., Iwuoha, E. & Okujeni, C. 2006 Treatment of acid mine drainage with fly ash: removal of major contaminants and trace elements. *J. Environ. Sci. Health-Part A* **41**(8), 1729–1747.

Gitari, W. M., Kaseke, C. & Nkuzani, B. B. 2011 Passive remediation of acid mine drainage using bentonite clay: a laboratory batch experimental study. *IMWA*, Aachen, Germany, pp. 325–330.

Johnson, D. B. & Hallberg, K. B. 2003 The microbiology of acidic mine waters. *Res. Microbiol.* **154**, 466–473.

Khandelwal, N., Singh, N., Tiwari, E. & Darbha, G. K. 2019 Novel synthesis of a clay supported amorphous aluminum nanocomposite and its application in removal of hexavalent chromium from aqueous 14 solutions. *RSC Advances* **9**(20), 11160–11169.

Water Practice & Technology Vol 16 No 2
doi: 10.2166/wpt.2021.014

Kopf, S. H., Henny, C. & Newman, D. K. 2013 Ligand-enhanced abiotic iron oxidation and the effects of chemical versus biological iron cycling in anoxic environments. *Environ. Sci. Technol.* **47**(6), 2602–2611.

Manecki, M., Maurice, P. A. & Traina, S. J. 2000a Kinetics of aqueous Pb reaction with apatites. *Soil. Sci.* **165**(12), 920–933.

Manecki, M., Maurice, P. A. & Traina, S. J. 2000b Uptake aqueous Pb by Cl-, F- and OH- apatite mineralogic evidence for nucleation mechanisms. *Am. Miner.* **85**(7–8), 932–942.

Maree, J. P. 1992 Treatment of acidic effluents with limestone instead of lime. *Wat. Sci. Technol.* **38**(1–2), 345–355.

Maree, J. P., Strobos, G., Greben, H., Netshidaula, E., Steyn, E., Christie, A., Gunther, P. & Waanders, F. B. 2004 Treatment of acid leachate from coal discard using calcium carbonate and biological sulphate removal. *Mine. Wat. & Environ.* **23**, 144–151.

Moore, J. W., Davies, W. G. & Collins, R. W. 1978 *Chemistry*. McGraw-Hill Inc., New York, NY, USA.

Nel, M., Waander, F. B. & Fosso-Kankeu, E. 2014 Adsorption potential of bentonite and attapulgite clays applied for the desalination of sea water Conference Report Cape Town. In: *6th International Conference on Green Technology*. Renewable Energy & Environmental Engineering North-West University.

Nermen, M., Nakhla, G. & Wan, W. 2009 Comparative assessment of hydrophobic and hydrophilic membrane fouling in wastewater applications. *J. of Membr. Sci.* **339**(1), 93–99.

Nriagu, J. O. 1984 Formation of stability of base metal phosphates in salts and sediments. In: *Phosphate Minerals* (Nriagu, J. O. & Moore, P. K. eds). Springer-Verlag, London, UK.

Ntwampe, I. O. 2013 *Paint Wastewater Treatment Using Fe^{3+} and Al^{3+} Salts*. PhD Thesis, The University of the Witwatersrand, South Africa.

Ntwampe, I. O., Hildebrandt, D. & Glasser, D. 2013a The effect of mixing on the treatment of paint wastewater with Fe^{3+} and Al^{3+} salts. *J. of Environ. Chem. and Ecotoxicol.* **5**(1), 7–16.

Ntwampe, I. O., Jewell, L. L., Hildebrandt, D. & Glasser, D. 2013b The effect of water hardness on paint wastewater treatment by coagulation-flocculation. *J. Environ. Chem. and Ecotoxicol.* **5**(3), 47–56.

Ntwampe, I. O., Waanders, F., Fosso-Kankeu, E. & Bunt, J. 2015a Reaction dynamics of iron and aluminium salts dosage in AMD using shaking as an alternative technique in the destabilization-hydrolysis process. *Int. J. Sci. Res.* **4**, 5–23.

Ntwampe, I. O., Waanders, F. B., Kosso-Kankeu, E. & Bunt, J. R. 2015b Turbidity removal efficiencies of clay and af-PFCl polymer of magnesium hydroxide in AMD treatment. *Int. J. Sci. Res.* **4**, 38–55.

Ntwampe, I. O., Waanders, F. B., Bunt, J. R. & Fosso-Kankeu, E. 2015c Chemical reactivity between $CaCO_3$ and $Ca(OH)_2$ in AMD with mixing and shaking techniques during the destabilization-hydrolysis of the AMD. *J. Chem. Eng. Mat. Sci.* **7**(3), 34–51.

Ntwampe, I. O. & Moothi, K. 2018 Investigation of the effect of a flocculent of bentonite clay with $MgCO_3$ in synthetic AMD treatment. *J. App. Chem. Sci.* **5**(2), 435–444.

Ntwampe, O. I. & Moothi, K. 2019 Reaction dynamics of bentonite clay, $FeCl_3$, $Al_2(SO_4)_3$ and Na_2CO_3 dosage in AMD using varying dispersion techniques. *J. Environ. Man.* **231**, 552–561.

Nzihou, A. & Sharrock, P. 2009 Role of phosphate in the remediation and reuse of heavy metal polluted wastes and sites. *Waste Biomass Valor.* **1**, 163–174.

Oladipo, A. A. & Gazi, M. 2014 Enhanced removal of CV by low cost alginate/acid activated bentonite composite beads; optimization and modeling using non-linear regression technique. *J. Wat. Proc. Eng.* **2**, 43–52.

Petrik, L. F., White, R. A., Klink, M. J., Somerset, V. S., Burgers, C. L. & Fey, M. V. 2003 Utilization of South African Fly Ash to Treat Acid Coal Mine Drainage, and Production of High Quality Zeolites from the Residual Solids. In: *Submission of International Ash Utilization Symposium*, October 20–22, 2003, Lexington, Kentucky, USA.

Sinha, P., Szilagyi, I., Ruiz-Cabello, F. J. M., Maroni, P. & Borkovec, M. 2013 Attractive forces between charged colloidal particles induced by multivalent ions revealed by confronting aggregation and direct force measurements. *J. Phys. Chem.* **4**(4), 648–652.

Strawn, D. G. & Sparks, D. L. 1999 The Use of XAFS to distinguish between inner- and outer-Sphere lead adsorption complexes on montmorillonite. *Journal of Colloid and Interface Science* **216**, 257–269.

Suzuki, T., Hatsushika, T. & Hayakawa, Y. 1981 Synthetic hydroxyapatites employed as inorganic cation-exchangers. *J. Chem. Soc. Faraday Trans.* **77**(5), 1059–1062.

Suzuki, T., Hatsushika, T. & Miyake, M. 1982 Synthetic hydroxyapatites as inorganic cation-exchangers, Part 2. *J. Chem. Soc. Faraday Trans.* **80**(12), 3605–3611.

Suzuki, T., Tshipaki, K. & Miyake, M. 1984 Synthetic hydroxyapatites as inorganic cation exchangers, Part 3. Exchange characteristics of lead ions (Pb^{2+}). *J. Chem Soc. Faraday Trans.* **80**(11), 3157–3165.

Syafalni Abdullah, R., Abustan, I. & Ibrahim, A. N. M. 2013 Waste water treatment using bentonite, the combination of bentonite-zeolite, bentonite-alum, and bentonite-limestone as adsorbent and coagulant. *Int. J. Environ. Sci.* **4**(3), 2013.

Tahir, S. S. & Naseem, R. 2007 Removal of Cr^{3+} from tannery waste water by adsorption onto bentonite clay. *Sep. and Purif. Technol.* **53**, 312–321.

van der Wat, J. G. 2011 *Desorption of Rare Earth Elements From Bentonite Clay via Acid Leaching*. PhD Thesis, North West University in South Africa.

Waanders, F. B. & Brink, M. C. 2010 The Rehabilitation of Acid Mine Effluents and Toxic Metal Pollution, emanating from gold mines in South Africa. In: *Proceedings XXV International Minerals Processing Conference, IMPC-2010*, Brisbane, Australia, pp. 4117–4126.

Water Practice & Technology Vol 16 No 2
doi: 10.2166/wpt.2021.014

Wei, X., Viadero Jr, R. C. & Bhojappa, S. 2008 Phosphorus removal by acid mine drainage sludge from secondary effluents of municipal wastewater treatment plants. *Wat. Res.* **42**, 3275–3284.

Weishaar, J. L., Aiken, G. R., Bergamaschi, B. A., Fram, M. S., Fujii, R. & Mopper, K. 2003 Evaluation of specific ultraviolet absorbance as an indicator of the chemical composition and reactivity of dissolved organic carbon. *Environ. Sci. Technol.* **37**(20), 4702–4708.

Zhao, X., Zhang, L. & Liu, D. 2012 Biomass recalcitrance. Part I: the chemical compositions and physical structures affecting the enzymatic hydrolysis of lignocellulose. *Biofuel. Bioprod. Biorefin.* **6**(4), 465–482.

First received 8 September 2020; accepted in revised form 7 February 2021. Available online 18 February 2021